Synthesis, Spectral Characterization and DFT Calculations of New Co(II) Complexes Derived from Benzimidazoles

Safavi Rad, Zahra; Pordel, Mehdi*[+]; Davvodnia, Abolghasem

Department of Chemistry, Mashhad Branch, Islamic Azad University, Mashhad, I.R. IRAN

ABSTRACT: *The synthesis, characterization and quantum-chemical investigations of two new Co(II) complexes derived from fluorescent benzimidazoles have been reported. Two new fluorescent heterocyclic ligands were synthesized from the reduction of imidazo[4',5':3,4]benzo[1,2-c]isoxazole derivatives, and characterized by elemental analyses, IR, mass, and NMR spectra. Coordination of the bidentate ligands with Co(II) cation produced orange complexes. The structures of the complexes have been established by spectral and analytical data as well as Job's method. The photophysical properties of the new ligands and Co(II) complexes were characterized by UV-Vis and fluorescence spectroscopies. An efficient charge transfer from the p-orbital of ligand to the Co(II) d-orbital could be proposed as the main reason for the color of the new complexes. To gain insight into geometry, spectral properties and the energy difference between the HOMO and LUMO frontier orbitals of the ligands and Co(II) complexes, the DFT calculations at the B3LYP/6-311++G(d,p) level were employed. The DFT-calculated spectral properties were in good agreement with the experimental values and confirmed the suitability of the optimized geometries for cobalt complexes.*

KEYWORDS: *Benzimidazole; Fluorescent ligands; Co(II) complex; UV-Vis and fluorescence spectroscopies; DFT.*

INTRODUCTION

Cobalt is an important trace element for all multi-cellular organisms as the active center of coenzymes called cobalamins. These coenzymes include vitamin B12 which is essential for mammals. Also, cobalt is an active nutrient for bacteria, algae, and fungi, and maybe a necessary nutrient for all live organisms [1–3]. In hence, the cobalt complexes display varying levels of biological activity such as antibacterial [4], antifungal [5], antivirus [6], antiproliferative [7,8] and anticancer [9–12]. They were also used as catalysts for a diverse range of organic reactions such as electrochemical [13], cross-coupling [14], polymerization [15], hydrogenation [16,17], Lewis acid catalyzed[18].

On the other hand, benzimidazoles have developed as significant heterocyclic compounds due to their presence in a wide range of bioactive compounds such as antiparasitic [19], anticonvulsant [20], analgesic [21], antihistaminic [22], antiulcer [23], antihypertensive [24], antiviral [25], anticancer [26], antifungal [27], anti-inflammatory and anticoagulants agents [28, 29] as well

***** *To whom correspondence should be addressed.*
+ E-mail: mehdipordel58@mshdiau.ac.ir
1021-9986/2019/5/111-120 10/$/6.00

as proton pump inhibitors [30]. Optimization of the benzimidazole substituents has resulted in many drugs like albendazole, mebendazole, thiabendazole as antihelmintics; omeprazole, lansoprazole, pantoprazole as proton pump inhibitors; astemizole as antihistaminic; enviradine as antiviral; candesarten cilexitil and telmisartan as antihypertensives. Also, benzimidazoles play an important role in determining the function of several biologically important metal complexes [31].

Based on these results, two new Co(II) complexes derived from their respective fluorescent benzimidazoles were synthesized. The optical properties of all compounds were also investigated by UV-Vis and fluorescence spectroscopies. Moreover, Density Functional Theory (DFT) calculations were performed to provide the optimized geometries, structural parameters, vibrational frequencies, and energy difference between the HOMO and LUMO frontier orbitals of the studied compounds.

EXPERIMENTAL SECTION

Equipment and Materials

Melting points were measured on an Electrothermal type-9100 melting-point apparatus. The FT-IR spectra were recorded on potassium bromide pellets using a Tensor 27 spectrometer and only noteworthy absorptions were listed. The ^{13}C NMR (75 MHz) and ^{1}H NMR (300 MHz) spectra were obtained on a Bruker Avance DRX-300 spectrometer.

Chemical shifts are reported in ppm downfield from TMS as internal standard; coupling constant is given as *J* value in Hz. The mass spectrum was recorded on a Varian Mat, CH-7 at 70 eV and ESI mass spectrum was measured using a Waters Micromass ZQ spectrometer. Elemental analysis was performed on a Thermo Finnigan Flash EA microanalyzer. Absorption and fluorescence spectra were recorded on Varian 50-bio UV-Visible spectrophotometer and Varian Cary Eclipse spectrofluorophotometer. UV–Vis and fluorescence scans were recorded from 200 to 1000 nm. Percentage of the Co(II) was obtained by using a Hitachi 2-2000 atomic absorption spectrophotometer.

All solvents were dried according to standard procedures. Compounds **2** [32] and **4 a,b** [33] were obtained according to the published methods. Other reagents were commercially available.

Computational methods

All calculations have been performed using the DFT method with the B3LYP hybrid functional [34] as implemented in the Gaussian 03 program package [35]. The 6-311++G(d,p) basis sets were employed except for the Co(II) where the LANL2DZ basis sets were used with considering its effective core potential. Geometry of the Co(II) complex was fully optimized, which confirmed to have no imaginary frequency of the Hessian. Geometry optimization and frequency calculation simulated the properties in the gas/solution phases.

The fully-optimized geometries were confirmed to have no imaginary frequency of the Hessian.

The solute-solvent interactions have been investigated using one of the self-consistent reaction field methods, i.e., the sophisticated Polarizable Continuum Model (PCM) [36].

General procedure for the synthesis of ligands 5a,b

Iron powder (0.89 g, 16 mmol) was added with stirring to a solution of **4a**,**b** (4 mmol) in EtOH (30 mL) and HCl (2 M, 2 mL). Then, the mixture was refluxed for 4 h and then poured into water. The precipitate was collected by filtration, washed with water, and air-dried to give crude **5a**,**b**.

(5-Amino-1-benzyl-1H-benzo[d]imidazol-4-yl) (phenyl) methanone (**5a, L1**) was obtained as shiny yellow needles (EtOH). m.p.: 192–194 °C; yield: 82%. ^{1}H NMR ($CDCl_3$): δ 5.29 (br s, 4H, $\underline{CH_2}$Ar and NH_2), 6.70 (d , *J* = 8.7 Hz, 1H, Ar H), 7.17–7.45 (m , 8H, Ar H), 7.56 (t, *J* = 7.2 Hz, 1H, Ar H), 7.70 (s, 1H, imidazole Ar H), 7.97 (d, *J* = 8.4 Hz, 2H, Ar H), 7.81 (d, *J* = 7.5 Hz, 2H, Ar H) ppm; ^{13}C NMR ($CDCl_3$): δ 48.9 ($\underline{C}H_2$Ar) , 111.5, 114.3, 115.3, 126.7, 127.0, 127.9, 128.3, 129.1, 129.8, 132.1, 135.4, 140.7, 142.6, 144.0, 145.8, 197.3 (C=O) ppm. IR (KBr): 3403, 3275 (NH_2), 1634 (C=O) cm^{-1}. MS (m/z) 327 (M^+). Anal. Calcd for $C_{21}H_{17}N_3O$ (327.4): C, 77.04; H, 5.23; N, 12.84. Found: C, 76.83; H, 5.19; N, 12.98.

*(5-Amino-1- benzyl- 1H-benzo[d] imidazole -4-yl)(4-chlorophenyl) methanone (***5b, L2***)* was obtained as a shiny yellow needles. m.p.: 194-195 °C. yield: 86%. ^{1}H NMR (DMSO-d_6): δ 5.21 (s, 2H, $\underline{CH_2}$Ar), 5.30 (br s, 2H, NH_2), 6.60 (d , *J* = 8.7 Hz, 1H, Ar H), 7.07–7.14 (m , 3H, Ar H), 7.26–7.31 (m , 5H, Ar H), 7.61 (s, 1H, imidazole Ar H), 7.64 (d, *J* = 6.9 Hz, 2H, Ar H) ppm; ^{13}C NMR ($CDCl_3$): δ 48.5 ($\underline{C}H_2$Ar), 110.9, 114.4, 115.3, 126.6,

127.3, 128.4, 128.5, 129.9, 129.3, 132.5, 136.8, 140.3, 142.5, 144.5, 145.9, 196.6 (C=O) ppm. IR (KBr): 3398, 3272 (NH_2), 1630 (C=O) cm^{-1}. MS (m/z) 363 (M^++2). Anal. Calcd for $C_{21}H_{16}ClN_3O$ (361.8): C, 69.71; H, 4.46; N, 11.61. Found: C, 69.53; H, 4.43; N, 11.96.

General procedure for the synthesis of the complexes 6a,b

Cobalt(II) nitrate hexahydrate (0.29 g, 1 mmol) was added to the yellow solution of ligand **5a,b** (2 mmol) in aqueous methanolic solution (15 mL, MeOH: H_2O, 10:90). The solution color changed to deep orange. The reaction continued for another 8 h at rt. The complex was isolated by evaporation of the solvent and washed with cold MeOH and then H_2O.

$[Co(L1)_2]$ $N_2O_6.2(H_2O)$ (**6a**): was obtained as an orange powder. m.p. > 300 ºC (decomp). IR (KBr): 3375, 3260 (NH_2), 1620 (C=O) cm^{-1}, ESI-MS (+) m/z (%): 713 $[Co(L1)_2]^{2+}$. Anal. Calcd for $C_{42}H_{38}CoN_8O_{10}$ (873.7): C, 57.74; H, 4.38; N, 12.82; Co, 6.74. Found: C, 57.30; H, 4.32; N, 12.34; Co, 5.75.

$[Co(L2)_2]$ $N_2O_6.2(H_2O)$ (**6b**): was obtained as an orange powder. mp > 300 ºC (decomp). IR (KBr): 3377, 3263 (NH_2), 1624 (C=O) cm^{-1}, ESI-MS (+) m/z (%): 781 $[Co(L2)_2]^{2+}$. Anal. Calcd for $C_{42}H_{36}Cl_2CoN_8O_{10}$ (942.6): C, 53.52; H, 3.85; N, 11.89; Co, 6.25. Found: C, 53.90; H, 3.94; N, 11.56; Co, 6.01.

RESULTS AND DISCUSSION

Synthesis and structure of the new ligands 5a,b and complexes 6a,b

Two new heterocyclic ligands were prepared according to the following manners. Initial reaction of 5-nitro-1*H*-benzimidazole (**1**) with benzyl chloride in KOH and DMF produced 1-benzyl-5-nitro-1*H*-benzimidazoles (**2)** [32]. The reaction of 1-benzyl-5-nitro-1*H*-benzimidazole with benzyl cyanide (**3a**) or (4-chlorophenyl)acetonitrile (**3b**) in basic MeOH solution led to the formation of 3-benzyl-8phenyl-3*H*-imidazo[4',5':3,4]benzo[1,2-*c*]isoxazole (**4a**) or 3-benzyl-8-(4-chlorophenyl)-3*H*-imidazo[4',5':3,4]benzo[1,2-*c*]isoxazole (**4b)** [33]. Finally, reduction of compounds **4a,b** in EtOH with Fe/HCl, provided the new heterocyclic *o*-amino-ketones (5-amino-1-benzyl-1*H*-benzo[*d*]imidazol-4-yl)(phenyl)methanone (**5a)** and (5-amino-1-benzyl-1*H*-benzo[*d*]imidazol-4-yl)(4-chlorophenyl)methanone (**5b)** in high yields (Scheme 1).

The structural assignments of new compounds **5a**,**b** were based on the analytical and spectral data. For example, in the ^1H NMR spectrum of compound **5b,** there is an exchangeable peak at δ 5.30 ppm attributed to the NH_2 group proton. Also, there are two doublet signals (δ = 6.60 and 7.64 ppm), two multiplet signals (δ = 7.07–714 and 7.26–731 ppm) and singlet signal (δ = 7.61 ppm) assignable to twelve protons of aromatic rings and a single signal (δ = 5.21) attributed to the benzylic CH_2 proton. Also, 17 different carbon atom signals were observed in the ^{13}C NMR spectrum of compound **5b**. Furthermore, the IR spectrum of compound **5b** in KBr showed a broad absorption band at 3398 and 3272 cm^{-1} assignable to NH_2 and 1630 cm^{-1} attributed to the C=O groups. The results of mass spectroscopy (*m*/*z* 363 $[M+2]^+$) and elemental analyses support the structure of **5b**.

The coordination of ligands **5a,b** with Co(II) gave orange complexes **6a,b** in aqueous methanolic solution. The stoichiometry of the complexes **6a,b** obtained by Job's method (Figs. S1 and S2, Supplementary Data: ML_2) [37] together with the elemental analysis results (Experimental section) proposed the formula $[Co(L)_2]$ $N_2O_6.2(H_2O)$ for the complexes **6a,b** (Fig. 1). Also, molecular ion peak at m/z 713 ($[Co(L1)_2]^{2+}$) and m/z 781 ($[Co(L2)_2]^{2+}$) strongly support the structure of the new complexes **6a** and **6b**, respectively.

Photophysical properties of the new ligands and complexes

New fluorescent heterocyclic ligands **5a,b,** and Co(II) complexes **6a,b** were characterized by UV-Vis and fluorescence spectroscopies in the wavelength range of 200–1000 nm. The absorption (5×10^{-5} M) and fluorescence emission (1×10^{-6} M) spectra of **5a,b** and Co (II) complexes **6a,b** were depicted in Fig. 2. Numerical spectral data were also presented in Table 1. Values of extinction coefficient (ε) were calculated as the slope of the plot of absorbance *vs* concentration. As seen in Fig. 1, the spectra of the complexes **6a,b** have an absorption maximum at 440 nm at which the ligands have no absorbance. An efficient charge transfer of an electron from p-orbital on the ligand to Co(II) d-orbital can be considered as the main reason for the color of the complexes explained as Ligand to-Metal charge transfer (LMCT) [38]. Furthermore, ligands **5a,b,** and cobalt

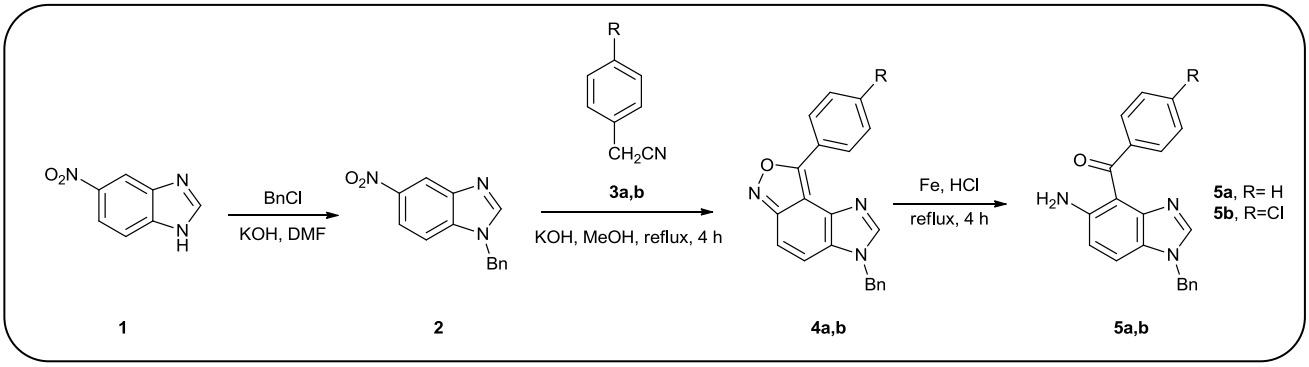

Scheme 1: Synthesis of the new ligands 5a,b.

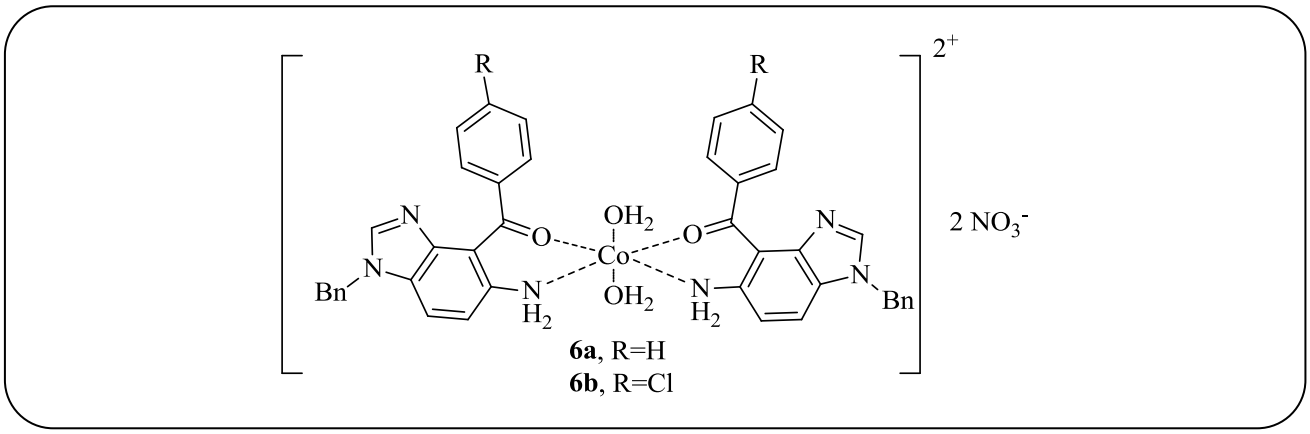

Fig. 1: The structure of new Co(II) complexes 6a,b.

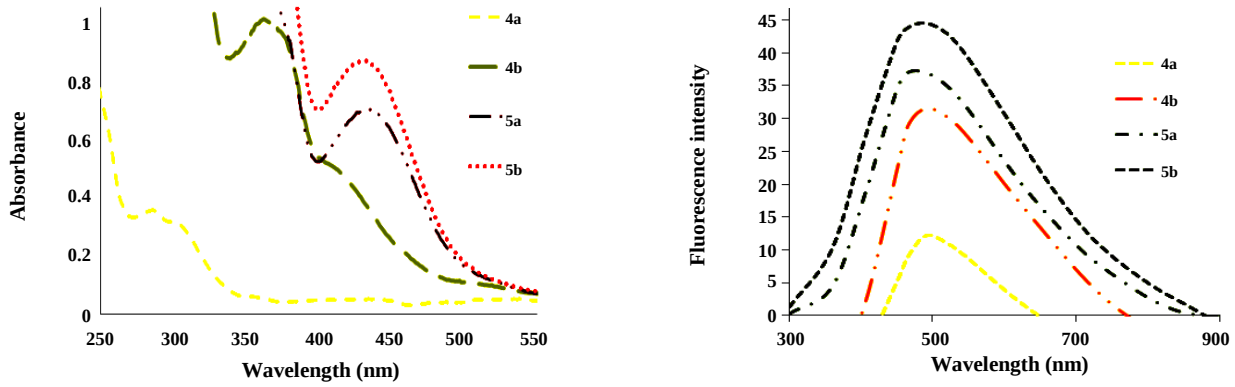

Fig. 2: The absorption (left) and fluorescence emission spectra of 5a,b and Co(II) complexes 6a,b in MeOH solution.

complexes **6a,b** produced fluorescent light in a dilute solution of MeOH (Fig. 2). The fluorescence quantum yields of the compounds were also determined and compared to fluorescein as a standard sample in 0.1 M NaOH and MeOH solution [39]. While the emission quantum yield of fluorescein is 0.79, the obtained emission quantum yields of the new compounds are around 0.45 – 0.69. As can be seen from Table 1, the extinction coefficient (ε) in **5b**, fluorescence intensity and the emission quantum yield in **6b** were the biggest values.

DFT Calculations

An octahedral geometry was proposed for Co(II) complexes **6a,b** based on our experimental results and

Table 1: Spectroscopic data for 5a,b and 6a,b at 298 K.

Dye	5a	5b	6a	6b
λ_{abs} (nm)[a]	295	360	440	440
$\varepsilon \times 10^{-3}$ [(mol L^{-1})$^{-1}$$cm^{-1}$][b]	7.4	20.0	14.0	17.4
λ_{flu} (nm)[c]	495	495	490	490
Φ_F[d]	0.45	0.51	0.61	0.69

a) Wavelengths of maximum absorbance (λ_{abs}). b) Extinction coefficient.
c) Wavelengths of fluorescence emission (λ_{flu}) with excitation at 350 nm. d) Fluorescence quantum yield

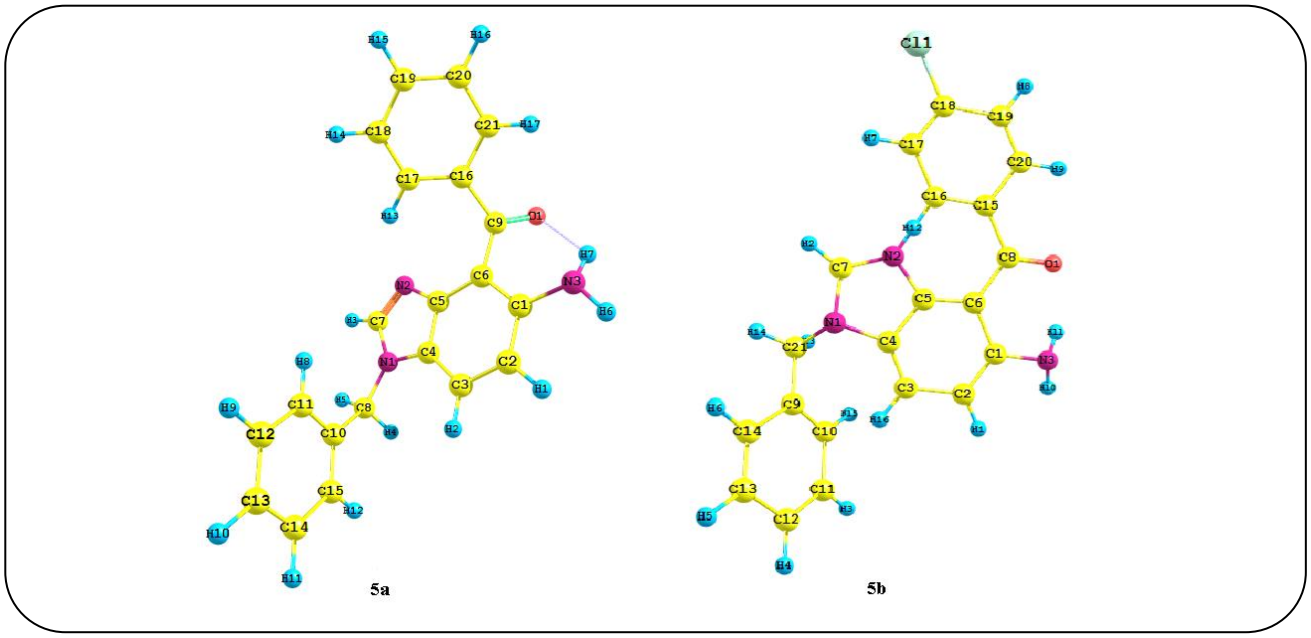

Fig. 3: The optimized geometry of the ligands 5a,b.

reported literatures [40, 41]. The optimized geometries and HOMO and LUMO frontier orbitals of fluorescent ligands **5a,b,** and Co(II) complex **6b** were obtained by DFT calculations at the B3LYP/6-311++G(d,p) level. The geometry of Co(II) complex **6b** was optimized in both the gas phase and MeOH as the solvent (PCM model). Figs. 3 and 4 show the optimized geometries of the ligands **5a,b,** and the complex **6b** respectively. Some of the calculated structural parameters of the Co(II) complex are listed in Table 2. Selected structural parameters of the ligands **4a,b** were depicted in Supplementary Data (Tables S1 and S2). In the optimized geometry of the complex **6b**, the ligand **5b** acts as a bidentate ligand and coordinates to the Co(II) *via* the nitrogen atom of the amine functional group and the oxygen atom of the carbonyl group. The aromatic rings of the ligand are approximately in the same plane. Two other positions of the complex are occupied by two H_2O molecules, which are *anti* to each other. The H_2O ligands are perpendicular to the square plane of the complex. The Co-O and Co-N bond lengths are collected in Table 2.

The vibrational modes of Co(II) complex **6b** were listed in Table 3, and compared to the experimental values. The atoms were numbered as shown in Fig.4. As seen in Table 3, there is a good agreement between the experimental data and DFT-calculated frequencies of the complex **6b**, which confirms the validity of the optimized geometry as a proper structure for the complex **6b**.

The 3D-distribution map for the highest-occupied-molecular orbital (HOMO) and the lowest-unoccupied-molecular orbital (LUMO) of the ligands **5a,b** and the complex **6b** was demonstrated in Fig. 5. As seen, the HOMO of the ligands was localized on the benzimidazole ring and the LUMO was mainly localized on the benzene

Table 2: Selected structural parameters of Co(II) complex 6b.

Bond	Bond length (A^0)	Angle	(°)	Dihedral angle	(°)
Co-O1	1.898	N1-Co-N5	179.90	O1-O2-O3-O4	179.544
Co-O4	1.898	O1-Co-O4	179.83	N3-O2-N6-O3	-0.048
Co-N3	1.970	O2-Co-O3	179.63	O1- Co-O4-N3	-92.752
Co-N6	1.970	Co-O1-C8	129.04	N3- Co-N6-O3	-7.207
Co-O3	2.318	O1-C8-C6	119.81	N6-C22-C27-C29	-3.551
Co-O2	2.323	Co-N3-C1	113.34	N4-C25-C26-N5	1.075
N3-C1	1.452	Co-O2-N3	36.837	N5-C28-N4-C42	-177.684
O1-C8	1.273	Co-O4-C29	129.032	C26-C27-C36-C41	0.419
N6-C22	1.452	C29-C36-C37	121.743	O1-C8-C15-C20	22.557
C27-C29	1.477	O4-C29-C27	119.754	C15-C8-C6-C5	38.811
C27-C26	1.420	C27-C26-N5	129.660	C5-N2-C7-N1	-0.153
C25-C26	1.424	N4-C28-N5	114.489	N2-C5-C6-C1	-175.84
C36-C38	1.410	N4-C42-C30	113.853	C7-N1-C21-C9	-123.135
C25 –N4	1.382	C42- C30-C35	120.808	C14-C9-C21-N1	56.569
C26-N5	1.373	C31-C30-C31	119.261	C10-C11-C12-C13	0.225
C28-N5	1.317	C30-C31-C32	120.445	C28-N4-C42-C30	-121.08
C28-N4	1.367	C32- C33-C34	119.864	C26-C27-C29-C36	-38.971
N4-C42	1.474	O1-C8-C15	119.864	Cl2-C39-C40-C41	-179.421
C42-C30	1.515	C8-C15-C16	121.744	C37-C38-C39-Cl2	-179.090
O4-C29	1.273	C8-C6-C5	122.362	O4-C29-C36-C41	-22.379

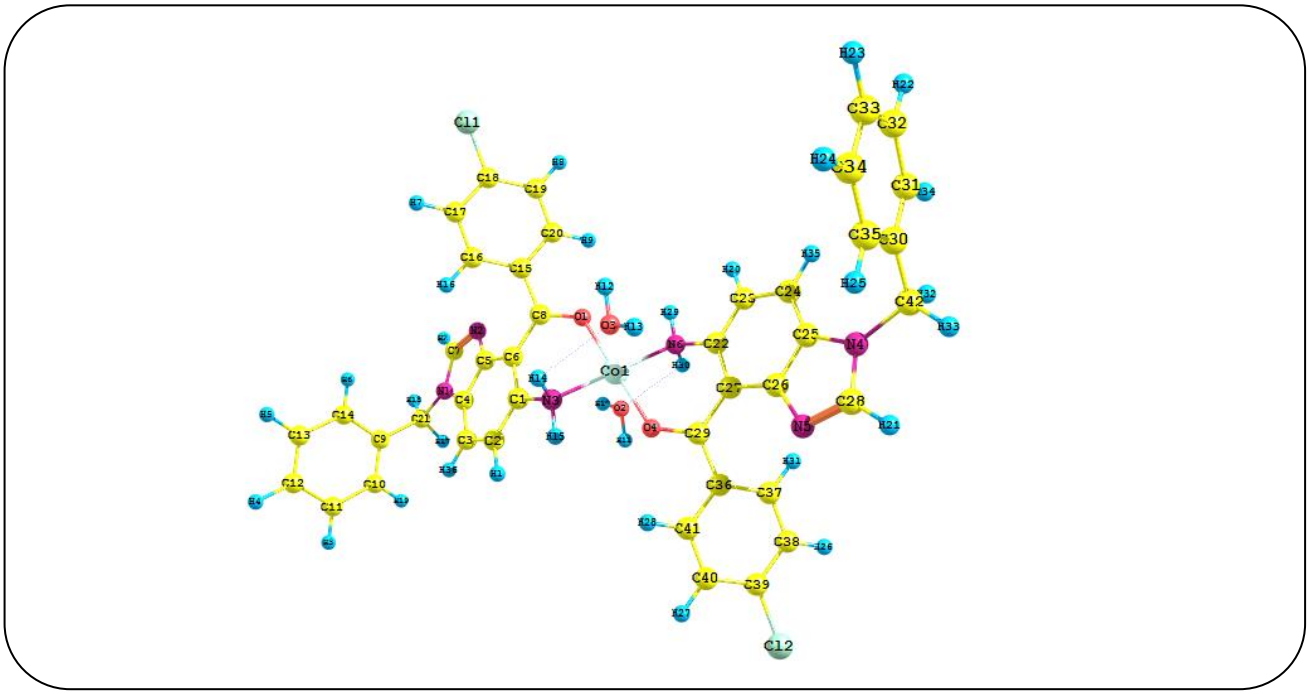

Fig. 4: The optimized geometry of the complex 6b.

Table 3: Selected experimental data and calculated IR vibrational frequencies (cm^{-1}) of Co(II) complex 6b.

Experimental frequencies	Calculated		
	Frequency	IR Intensity D(10^{-4}esu^2 cm^2)	Vibrational assignment
651 (w)	669	392	υ_{sym}(Co-N)
706 (w)	726	82	υ_{asym}(Co-N)
963 (m)	923	178	δ_{op}(C-H) aromatic
1194 (s)	1060	603	υ(C-Cl)
1285 (m)	1245	136	υ(C1-N3, C22-N6)
1382 (m)	1334	1829	υ_{asym} (C4-C5-N2) + υ_{asym} (C25-C26-N5)
1454 (s)	1413	513	υ(C=C, C=N) of the aromatic rings
	1458	47	υ(C21-C9)+ υ(C42-C30)
	1471	256	υ(C=N) of the aromatic rings + υ(C42-N4, C21-N1)
	1482	62	υ(C=N) of the aromatic rings + υ(C22-N6, C1-N3)
1624 (s)	1526	527	υ(C=C) of the aromatic rings
	1569	4100	δ_{sci}(H-O-H) of the H_2O ligands
	1638	322	υ(C=C) of the benzene rings
	1657	16	υ(C=C) of 1 moiety
2361 (m)	3078-3185	21-12	υ_{sym} (C-H) aliphatic
	3078-3126	21-3	υ_{asym} (C-H) aliphatic
	3185-3224	12-2	υ(C-H) aromatic
3381 (vs,br)	3539	19	υ(C28-H21)) + υ(C7-H2)
	3771	7	υ_{sym} (O-H) of the H_2O ligands
	3877	51	υ_{asym} (O-H) of the H_2O ligands

Abbreviation: op, out-of-plane; ip, in-plane; w, weak; m, medium; s, strong; vs, very strong; br, broad; sh, shoulder.

and benzimidazole rings. Since, electron transition from the HOMO to the LUMO was $\pi \rightarrow \pi^*$ transition in the ligands **5a,b**. On the other hand, the HOMO and LUMO frontier orbitals of the complex **6b** were mainly localized on the benzimidazole ring and Co atom, respectively. It implies that the electron transition from the HOMO orbital to the LUMO orbital is Ligand to-Metal charge transfer (LMCT) [38].

Energy gaps between the HOMO and LUMO ($\Delta\varepsilon = \varepsilon_{LUMO} - \varepsilon_{HOMO}$) of **5a**, **5b** and **6b** are 3.96 eV (313 nm), 3.60 eV (345 nm) and 2.95 eV (420 nm), compared with the experimental values of 295, 360 and 440 nm, respectively.

CONCLUSIONS

In this work, two new fluorescent heterocyclic ligands were synthesized from the reduction of imidazo [4',5':3,4]benzo[1,2-*c*]isoxazole derivatives. Coordination of the ligands to Co(II) cation gave orange complexes. The structures of the complexes have been established by spectral, analytical data and Job's method, and an octahedral geometry was proposed for the complexes. Fluorescent ligands and cobalt complexes were spectrally characterized by UV-Vis and fluorescence spectroscopies. Results revealed that ligands and Co(II) complexes generate fluorescent light in dilute solution of MeOH. The DFT methods were employed to gain a deeper insight into geometry and spectral properties of the new compounds. The DFT-calculated vibrational modes of Co(II) complexes are in good agreement with the experimental values, which confirm the suitability of the optimized geometries for the complexes. Besides, energy gaps between the HOMO and LUMO of ligands

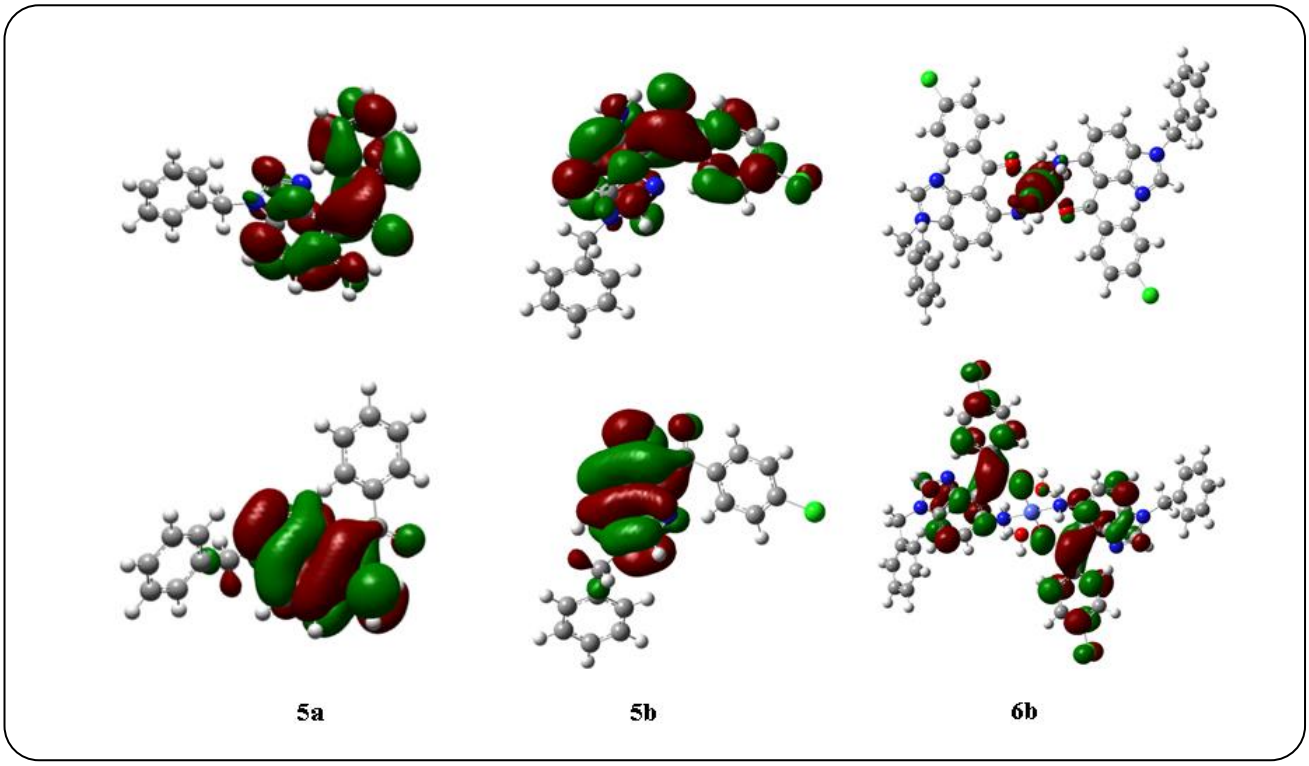

Fig. 5: The HOMO (down) and LUMO (up) frontier orbitals of 5a,b, and Co(II) complex 6b.

and Co(II) complexes were obtained and their 3D-distribution map revealed that electron transitions from HOMO to LUMO in the ligands and the complexes were $\pi \rightarrow \pi^*$ and LMCT transitions, respectively.

Acknowledgment

We would like to express our sincere gratitude to the Research Office, Mashhad Branch, Islamic Azad University, Mashhad-Iran, for financial support of this work.

Received : May 28, 2018 ; Accepted :Aug. 13, 2018

REFERENCES

[1] Li J., Wang J., Wang D., Guo G., Yeung K.W., Zhang X., Liu X., Band Gap Engineering of itania Film through Cobalt Regulation for Oxidative Damage of Bacterial Respiration and Viability, *ACS Appl. Mater. Interfaces*, **9**(33): 27475-27490 (2017).

[2] Goleij M., Fakhraee H., Response Surface Methodology Optimization of Cobalt (II) and Lead (II) Removal from Aqueous Solution Using MWCNT-Fe3O4 Nanocomposite. *Iran. J. Chem. Chem. Eng. (IJCCE)*, **36**(5): 129-141 (2017).

[3] Hartikainen E.S., Hatakka A., Kahkonen M.A., Impact of C admium., Chromium., Cobalt., Lithium and Manganese to the Growth of Fungi and Production of Enzymes, *Expert Opin. Environ. Biol.*, **2**(3): 1-7 (2013).

[4] Sethi R., Ahuja M., Synthesis., Characterization and Antibacterial Activity of Cobalt Complex of 2-Pyrazoline with Pyridinyl Moiety, *Int. J. Pharm. Tech. Res.*, **9**(1): 35-40 (2016).

[5] Canpolat E., Sahal H., Kaya M., Gur S., Synthesis, Characterization, Antibacterial and Antifungal Activities Studies of Copper (II),Cobalt (II) and Zinc (II) Complexes of the Schiff base Ligand Derived from 4, 4-diaminodiphenylether, *J. Chem. Soc. Pak.*, **36**(1): 106-112 (2014).

[6] Mil'grom A.E., Chegolya A.S., Filippova A.V., Vladyko G.V., Karako N.I., Synthesis and Antivirus Activity of Unprotonated Complex Salts of Amino Acids with Nickel and Cobalt. *Pharm. Chem. J.*, **18**(3): 179-182 (1984).

[7] Jayaraju D., Gopal Y.V., Kondapi A.K., Topoisomerase II Is A Cellular Target For Antiproliferative Cobalt Salicylaldoxime Complex, *Arch. Biochem. Biophys.*, **369**(1): 68-77 (1999).

[8] Wang N., Lin Q.Y., Feng J., Zhao Y.L., Wang Y.J., Li S.K., Crystal Structures., DNA Interaction and Antiproliferative Activities of the Cobalt (II) and Zinc (II) Complexes of 2-amino-1., 3., 4-thiadiazole with Demethylcantharate, *Inorganica. Chim. Acta*., **363** (13):3399-3406 (2010).

[9] Munteanu C.R., Suntharalingam K., Advances in Cobalt Complexes as Anticancer Agents, *Dalton Trans*., **44 (**31):13796-13808 (2015).

[10] Ghosh P., Chowdhury A.R., Saha S.K., Ghosh M., Pal M., Murmu N.C., Banerjee P., Synthesis and Characterization of Redox Non-innocent Cobalt (III) Complexes of a O., N., O Donor Ligand: Radical Generation., Semi-Conductivity., Antibacterial and Anticancer Activities, *Inorganica Chim. Acta*., **429:**99-108 (2005).

[11] King A.P., Gellineau H.A., Ahn J.E., MacMillan S.N., Wilson J.J., Bis (thiosemicarbazone) Complexes of Cobalt (III). Synthesis., Characterization., and Anticancer Potential, *Inorg. Chem*., **56**(11): 6609-6623 (2017) .

[12] Banerjee S., Chakravarty A.R., Metal Complexes of Curcumin for Cellular Imaging., Targeting., and Photoinduced Anticancer Activity, *Acc. Chem. Res*., **48**(7): 2075-2083 (2015).

[13] Wasylenko D.J., Ganesamoorthy C., Borau-Garcia J., Berlinguette C.P., Electrochemical Evidence for Catalyticwater Oxidation Mediated by a High-valent Cobalt Complex, *Chem. Commun*., **47**(14): 4249-4251 (2011).

[14] Farmacijo F.Z., Koren Ž., "Sinteza In Biokemijsko Preizkušanje Zaviralcev Benzoatne 4-Monooksigenaze Kot Novih Protiglivičnih Spojin", Doctoral Dissertation, Univerza v Ljubljani, Fakulteta za Farmacijo, (2014).

[15] Peng C.H., Yang T.Y., Zhao Y., Fu X., Reversible Deactivation Radical Polymerization Mediated by Cobalt Complexes: Recent Progress and Perspectives, *Org. Biomol. Chem*., **12** (43): 8580-8587 (2014).

[16] Srimani D., Mukherjee A., Goldberg A.F., Leitus G., Diskin-Posner Y., Shimon L.J., Ben David Y., Milstein D., Cobal Catalyzed Hydrogenation of Esters to Alcohols: Unexpected Reactivity Trend Indicates Ester Enolate Intermediacy, *Angew. Chem. Int*., **54**(42):12357-12360 (2015).

[17] Friedfeld M.R., Margulieux G.W., Schaefer B.A., Chirik P.J., Bis (phosphine) Cobalt Dialkyl Complexes for Directed Catalytic Alkene Hydrogenation, *J. Am. Chem. Soc*., **136** (38): 13178-13181 (2014).

[18] Rulev Y.A., Larionov V.A., Lokutova A.V., Moskalenko M.A., Lependina O.G., Maleev V.I., North M., Belokon Y.N., ChiralCobalt (III) Complexes as Bifunctional Brønsted Acid–Lewis Base Catalysts for the Preparation of Cyclic Organic Carbonates, *Chem. Sus. Chem*., **9** (2): 216-222 (2016).

[19] Flores-Carrillo P., Velázquez-López J.M., Aguayo-Ortiz R., Hernández-Campos A., Trejo-Soto P.J., Yépez-Mulia L., Castillo R., Synthesis, Antiprotozoal Activity, and Chemoinformatic Analysis of 2-(methylthio)-1H-benzimidazole-5-carboxamide Derivatives: Identification of new Selective Giardicidal and Trichomonicidal Compounds, *Eur. J. Med. Chem*., **137**: 211-220 (2017).

[20] Siddiqui N., Alam M.S., Ali R., Yar M.S., Alam O., Synthesis of new benzimidazole and phenylhydrazinecarbothiomideHybrids and Their Anticonvulsant Activity, *J. Med. Chem*., **25** (7): 1390-1402 (2016).

[21] Siddiqui N., Alam M.S., Sahu M., Yar M.S., Alam O., Siddiqui M.J., Antidepressant., Analgesic Activity and SAR Studies of Substituted benzimidazoles, *Asian J. Pharm. Clin. Res*., **6** (3): 170-174 (2016).

[22] Ding A.J., Wu G.S., Tang B., Hong X., Zhu M.X., Luo H.R., Benzimidazole Derivative M084 Extends the Lifespan of Caenorhabditis Elegans in a DAF-16/FOXO-dependent Way, *Mol. Cell Biochem*., **426**(1-2): 101-109 (2017).

[23] Saini S., Dhiman N., Mittal A., Kumar G., Synthesis and Antioxidant Activity of the 2-methyl benzimidazole, *J. Drug Deliv. Ther*., **6**(3): 100-102 (2016).

[24] Zhang Y., Xu J., Li Y., Yao H., Wu X. Design., Synthesis and Pharmacological Evaluation of Novel NOReleasing Benzimidazole Hybrids as Potential Antihypertensive Candidate, *Chem. Biol. Drug Des*., **85** (5): 541-548 (2015).

[25] Vausselin T., Séron K., Lavie M., Mesalam A.A., Lemasson M., Belouzard S., Fénéant L., Danneels A., Rouillé Y., Cocquerel L., Foquet L., Identification of A New benzimidazole Derivative as an Antiviral Against Hepatitis C Virus, *J. Virol*., **90**(19): 8422-8434 (2016).

[26] Kumar A., Kumar A., Gupta RK., Paitandi R.P., Singh K.B., Trigun S.K., Hundal M.S., Pandey DS., Cationic Ru (II)., Rh (III) and Ir (III) Complexes Containing Cyclic π-perimeter and 2-aminophenyl benzimidazole Ligands: Synthesis., Molecular Structure., DNA and Protein Binding., Cytotoxicity and Anticancer Activity, *J. Organomet. Chem*., **801**: 68-79 (2016).

[27] Keller P., Müller C., Engelhardt I., Hiller E., Lemuth K., Eickhoff H., Wiesmüller K.H., Burger-Kentischer A., Bracher F., Rupp S., An Antifungal benzimidazole Derivative Inhibits Ergosterol Biosynthesis and Reveals Novel Sterols, *Antimicrob. Agents Chemother*., **59**(10): 6296-6307 (2015).

[28] Gaba M., Singh S., Mohan C., Benzimidazole: An Emerging Scaffold for Analgesic and Anti-inflammatory Agents, *Eur. J. Med. Chem*., **76**:494-505 (2014).

[29] Yang H., Ren Y., Gao X., Gao Y., Synthesis and Anticoagulant Bioactivity Evaluation of 1., 2., 5-trisubstituted benzimidazole Fluorinated Derivatives, *Chem. Res. Chin. Univ*., **32**(6):973-978 (2016).

[30] Van Oosten M.J., Silletti S., Guida G., Cirillo V., Di Stasio E., Carillo P., Woodrow P., Maggio A., Raimondi G., A Benzimidazole Proton Pump Inhibitor Increases Growth and Tolerance to Salt Stress in Tomato, *Front. Plant. Sci*., **8**:1-14 (2017).

[31] Bansal Y., Silakari O., The Therapeutic Journey of benzimidazoles: A Review, *Bioorg. Med. Chem*., **20**(21): 6208-6236 (2012).

[32] Shintou T., Kikuchi W., Mukaiyama T., Efficient Method for the Preparation of Carboxylic Acid Alkyl Esters or Alkyl Phenyl Ethers by A New-type of Oxidation–reduction Condensation using 2., 6-dimethyl-1., 4-benzoquinone and alkoxydiphenylphosphines, *B. Chem. Soc. Jpn*., **76**(8): 1645-1667 (2003).

[33] Rahimizadeh M., Pordel M., Bakavoli M., Rezaeian S., Eshghi H., Synthesis of A New Heterocyclic System—Fluoreno [1., 2-d] imidazol-10-one, *Can. J. Chem*., **87**(6): 724-728 (2009).

[34] Lee C., Yang W., Parr RG., Development of the Colle-Salvetti Correlation-energy Formula into a Functional of the Electron Density, *Phys. Rev. B*., **37**(2): 785-789 (1998).

[35] Frisch M.J., Trucks GW., Schlegel H.B., GAUSSIAN 03, Gaussian, Inc., Pittsburgh, PA, 11 JB Foresman and A. Frisch (2003).

[36] Cammi R., Tomasi J., Remarks on the Use of the Apparent Surface Charges (ASC) methods in Solvation Problems: Iterative Versus Matrix inversion Procedures and the Renormalization of the Apparent Charges, *J. Comput. Chem*., **16**(12): 1449-1458 (1995).

[37] Vosburgh W.C., Cooper G.R., Complex ions. I. The Identification of Complex Ions in Solution by Spectrophotometric Measurements, *J. Am. Chem. Soc*., **63**(2): 437-442 (1941).

[38] Saureu S., de Graaf C., TD-DFT Study of the Light-induced Spin Crossover of Fe (III) Complexes, *Phys. Chem. Chem. Phys*., **18**(2): 1233-1244 (2016).

[39] Umberger J.Q., LaMer V.K., The Kinetics of Diffusion Controlled Molecular and Ionic Reactions in Solution as Determined by Measurements of the Quenching of Fluorescence1, *J. Am. Chem. Soc*., **67**(7): 1099-1109 (1945).

[40] Johnston H.M., Palacios P.M., Pierce B.S., Green K.N., Spectroscopic and solid-state Evaluations of Tetra-aza Macrocyclic Cobalt Complexes with Parallels to the Classic Cobalt (II) Chloride Equilibrium, *J. Coord. Chem*., **69**(11-13): 1979-1989 (2016).

[41] Habib F., Luca O.R., Vieru V., Shiddiq M., Korobkov I., Gorelsky S.I., Takase M.K., Chibotaru L.F., Hill S., Crabtree R.H., Murugesu M., Influence of the Ligand Field on Slow Magnetization Relaxation Versus Spin Crossover in Mononuclear Cobalt Complexes, *Angew. Chem. Int. Ed*., **52**(43): 11290-11293 (2013).